Article

Not peer-reviewed version

Paracetamol Removal from Aqueous Media Through Fenton Reaction Using ZSM-5 Zeolite Produced from Fly-Ash

Nuno Horta , Sofia Martins , Hugo F. Silva , Nelson Nunes , Ana S. Mestre , Ana P. Carvalho , Angela Martins *

Posted Date: 31 December 2025

doi: 10.20944/preprints202512.2787.v1

Keywords: fly-ash; ZSM-5 zeolite; paracetamol; Fenton reaction; kinetic parameters

 doi:10.20944/preprints202512.2787.v1

Article

Paracetamol Removal from Aqueous Media Through Fenton Reaction Using ZSM-5 Zeolite Produced from Fly-Ash

Nuno Horta [1], Sofia Martins [1], Hugo F. Silva [1,2], Nelson Nunes [1,2], Ana S. Mestre [2,3], Ana P. Carvalho [2,3] and Angela Martins [1,2,*]

[1] Departamento de Engenharia Química, Instituto Superior de Engenharia de Lisboa, IPL, R. Conselheiro Emídio Navarro, 1, 1959-007 Lisboa, Portugal

[2] Centro de Química Estrutural, Faculdade de Ciências, Institute of Molecular Sciences, Universidade de Lisboa, Campo Grande, 1749-016 Lisboa, Portugal

[3] Departamento de Química e Bioquímica, Faculdade de Ciências Universidade de Lisboa, Ed.C8, Campo Grande, 1749-016 Lisboa, Portugal

* Correspondence: amartins@deq.isel.ipl.pt

Abstract

The purpose of this study is the exploration of the catalytic performance of ZSM-5 zeolite produced from iron rich fly-ash without further addition of iron sites, in the removal of paracetamol through heterogenous Fenton reaction. The structural and textural characterization by powder X-ray diffraction and N_2 adsorption isotherms showed that pure ZSM-5 phase was synthesized, but lower crystallinity and textural parameters were obtained when confronting with commercial ZSM-5. The XPS analysis revealed the presence of significant amounts of iron as well as yttrium, which increased the electronic properties of the samples surface, when compared with iron impregnated commercial ZSM-5. The catalytic reaction was followed through UV-spectroscopy and kinetic models were applied to the data, with the best fit obtained for pseudo-first-order model. All fly ash-based zeolites present enhanced paracetamol removal when compared with commercial iron loaded ZSM-5 which may be attributed to the more disorganized structure, able to accommodate large paracetamol species (dimers). On the other hand, the effect of yttrium on the electronic properties of iron sites may increase the formation of •OH radicals, thus increasing the removal rate of paracetamol.

Keywords: fly-ash; ZSM-5 zeolite; paracetamol; Fenton reaction; kinetic parameters

1. Introduction

The supply of drinking water is one of the greatest concerns of industrialized societies. Among persistent organic pollutants (POPs), pharmaceuticals are of particular concern due to their increasing consumption and unclear cumulative effect both in human health and environment [1,2]. Paracetamol (PA), also designated as acetaminophen, is a drug used to treat fever and mild to moderate pain. PA toxicity was evaluated in some hosts like bacteria, algae, protozoan and fishes, showing that long-term exposure to this medicine can cause genetic code damage, oxidative degradation of lipids, and denaturation of protein in cells [3,4] Thus, the removal of PA and/or its degradation products from wastewater is mandatory to avoid harmful health effects on living beings and environment. Several studies point out that even after conventional wastewater treatment processes, a significant amount of PA may remain in the environment either in their original form or as by-products; therefore, more efficient processes are required to remove/convert it into innocuous compounds [5]. In the last decades, several studies have shown that advanced oxidation processes (AOPs) are effective for the degradation of organic molecules, including pharmaceutical compounds. AOPs are based on the generation of highly reactive and non-selective oxidant species, such as

 doi:10.20944/preprints202512.2787.v1

hydroxyl radical, •OH , that can transform organic molecules into simple H_2O and CO_2, as final products [2,3]. A typical homogeneous Fenton reaction follows a free radical mechanism, involving the interaction between Fe^{2+} and H_2O_2 in acidic conditions. The •OH radical species are then generated, thus promoting the degradation of a wide range of organic molecules, according to Equations (1) to (3)

$$Fe^{2+} + H_2O_2 \rightarrow Fe^{3+} + OH^- + {}^{\bullet}OH \quad (1)$$

$$Fe^{3+} + H_2O_2 \rightarrow {}^{\bullet}OOH + Fe^{2+} + H^+ \quad (2)$$

$$RH + {}^{\bullet}OH \rightarrow H_2O + {}^{\bullet}R \rightarrow \text{Degradation} \rightarrow \text{Mineralization} \quad (3)$$

The main drawback of homogeneous Fenton reaction is the need to operate in a very acidic environment, typically at pH between 2 and 4, to avoid the precipitation of inactive iron oxyhydroxides species [6], forming iron sludges. The costs associated with the removal of the sludges, the effluent treatment and the catalysts loss, make the quest for alternative heterogeneous catalysts most appealing. Several heterogeneous iron-based catalysts have been studied, allowing operating in a wider pH range, with reuse possibility. [7,8]. Fe-containing zeolites are among the most interesting candidates to replace homogeneous catalysts, due to their crystalline, ordered porous structure and ability to anchor metal species both at the external and inner surface. Thus, hetero-Fenton reactions occur, according to Equation (4), where Z-Fe^{2+} and Z-Fe^{3+} are the iron species supported at the zeolite [9].

$$Z\text{-}Fe^{2+} + H_2O_2 \rightarrow Z\text{-}Fe^{3+} + OH^- + {}^{\bullet}OH \quad (4)$$

Several studies report the use of iron loaded zeolites as Fenton and photo-Fenton catalyst for the removal of a wide range of organic pollutants [9–12]. The catalytic performance of these materials strongly depends on the type of zeolite structure and the Si/Al ratio [9]. On the other hand, high iron loadings may result on important losses of microporous volume and clogging of pore openings, which hinders access to the inner porosity [5]. Iron loaded ZSM-5 (MFI structure), one of the most used zeolites as heterogeneous catalyst or catalyst supports, has been standing out as an effective Fenton or photo-Fenton catalyst [5,12]. Recently, modified Fe-ZSM-5 was studied in the removal of methylene blue dye [11]. In this case, prior to iron loading, the commercial ZSM-5 was modified through desilication followed, in some cases, by acid leaching. The generated mesoporosity facilitated diffusion, leading to an improved catalytic performance, but also increased the catalysts preparation costs. Accordingly, low cost and effective synthesis procedures of iron loaded zeolites are desired.

Fly ash (FA) is a by-product of coal combustion in thermal power plants, with a worldwide production of about 780 million tonnes, but a low recycling rate of around 25 %, mostly as an additive for cement (≈ 20%)[13,14]. Therefore, fly ash is considered a hazardous waste, and the disposal of large amounts of this material has become a serious environmental concern. Accordingly, from the perspective of Circular Economy, FA is still a resource to be explored. The chemical composition of FA depends on the coal origin and technological processes used in thermal power plants. According to Vassilev and Vassileva [15] about 316 and 188 minerals or mineral groups have been identified in coals and respective FAs. The chemical composition of FA includes, in order of decreasing amounts, oxygen, silicon, aluminum, calcium, iron, carbon, potassium, magnesium and sulfur. Rare earth elements (REE) have also been detected. The presence of these elements has been highlighted given the scarcity and critical need for various industry sectors like automotive, electronics, energy, etc., raising the feasibility of extracting REE from fly ashes [16,17].

Since all fly ash materials are rich in mineral phases containing Si and Al, which are the main composition of zeolites, the process of turning FA into zeolites has been the focus of growing interest, as it enables the reduction of waste disposal and its conversion into a valuable product. The synthesis of several zeolite structures has been reported [18,19], including ZSM-5 [20]. The synthesis of zeolites

 doi:10.20944/preprints202512.2787.v1

from FA requires the digestion in alkaline media of the insoluble glass phase and crystalline phases such as mullite and quartz to transform the building blocks into aluminosilicate framework typical of zeolites. [18,21]. However, this process brings some concern since it could induce mobilization of some toxic heavy metals, causing contamination of the environment. This subject was investigated by Feng et al. [18] who concluded that less than 20% of heavy metals (copper, chromium and lead) from FA went to wastewater, whereas the rest along with almost all cadmium, iron, and nickel were incorporated into the synthesized zeolite structures. In addition, it was found that those chemical elements remained in the zeolite structure, without further leaching, whatever the pH conditions, therefore the synthesized zeolites are safe for applications. Within this scope, the present study deals with the synthesis of ZSM-5 zeolite from FA, pretending that chemical elements, such as iron, present on the raw FA are also immobilized at the zeolite structure and behave as active sites for the removal of paracetamol through Fenton reaction.

2. Results

2.1. Materials Characterization

The fly ash (FA) used in this study were supplied by a Portuguese power plant, which burned a bituminous coal type originating from Colombia. The characterization of FA sample was performed in a previous study [22], where the mineral content was examined, as well as, the leaching effect when FA contacted with aqueous media. The FA major components are aluminum and silicon, with a Si/Al ratio around 3 and a total iron content of about 4.3 wt.% (0.8 mmol g^{-1}). The data of the aqueous leachate showed that FA can be safely used without significant release of harmful elements through lixiviation [22].

ZSM-5 zeolite was synthesized from fly ash, through a 2-step synthesis procedure, based on the literature [23,24]. To optimize the synthesis, the influence of the amount of structuring agent tetrapropylammonium bromide (TPABr) added during the alkaline digestion step, and the time spent in the autoclave for the hydrothermal treatment was evaluated. To complete the previous characterization, the surface analysis of the main components through X-ray photoelectron spectroscopy (XPS) was performed on the raw FA, and also on the zeolite sample FA_ZSM5_006_72, i.e., synthesized with 1 SiO_2 : 0.06 TPABr ratio, during 72 h in the autoclave at 160 ^{0}C (see detailed synthesis procedure ahead), and a commercial ZSM-5 zeolite loaded with the same iron amount as detected on FA, Fe/ZSM5_C. The survey spectra are depicted in Figure 1.

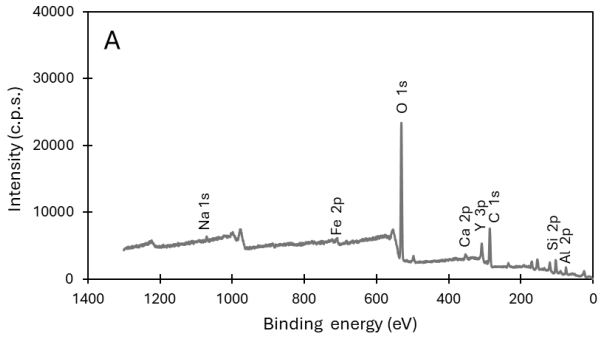

 doi:10.20944/preprints202512.2787.v1

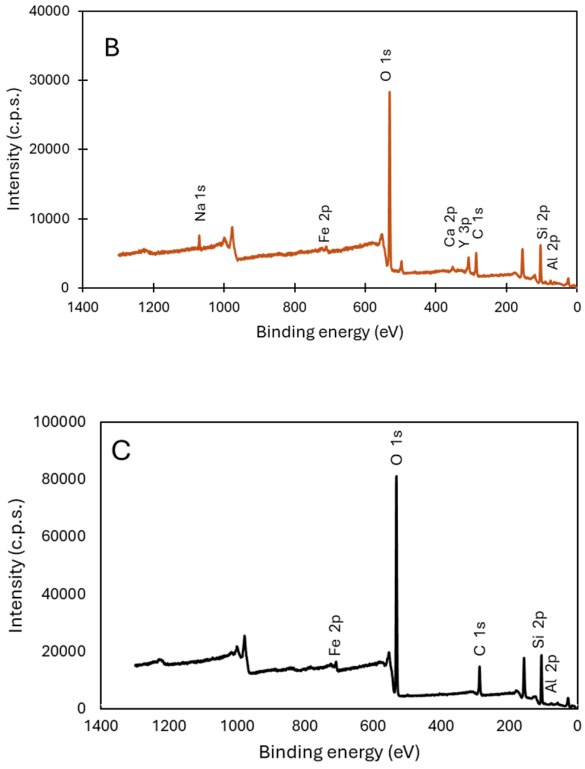

Figure 1. XPS survey spectrum of samples FA (A), FA_ZSM5_006_72 (B) and Fe/ZSM5_C (C).

As expected, oxygen, silicon, carbon, iron, and aluminum were detected in all samples, including the iron that was introduced on the commercial ZSM-5. For FA and the derived zeolite sample FA_ZSM5_006_72, other elements such as sodium, calcium and yttrium were also detected. It is also noted that these elements are present in both FA and FA-ZSM5_006_72 sample meaning that the leaching for the synthesis media is not significant and the elements were incorporated into the zeolite structure. Table 1 shows the correspondent surface composition of FA, FA_ZSM5_006_72 and Fe/ZSM5_C samples.

Table 1. Surface contents determined from XPS atomic percentages for FA, Fa_ZSM5_006_72, and Fe/ZSM5_C samples.

Element (mmol g^{-1})[1]	FA	FA_ZSM5_006_72	Fe_ZSM5_C
O	24.3	23.7	24.5
C	18.9	8.7	9.6
Si	7.7	20.3	16.2
Al	5.3	2.4	0.7
Na	0.4	0.6	-
Fe	0.3	0.4	0.4
Y	1.4	0.8	-

[1]mmol X/g = atomic % X / (∑[atomic%(i) × Ar(i)].

As expected, oxygen, carbon, silicon and aluminum are the main elements. Sodium, iron and yttrium are present in substantially lower amounts. When confronting the surface composition of FA and the derived zeolite sample, FA_ZSM5_006_72, a decrease in carbon content is observed, attributed to the calcination step, and an increase in silicon due to the addition of SiO_2 during zeolite synthesis. As mentioned before, the contents in sodium, iron and yttrium were transferred from FA

 doi:10.20944/preprints202512.2787.v1

to FA_ZSM5_006_72 zeolite, which is particularly relevant in the case of iron since the surface amount present on Fe/ZSM5_C is identical, which seems to indicate that the further addition of iron to the FA derived sample may not be required. This is especially important since the desired application of the produced zeolites is Fenton reaction, where iron species are the active sites. However, the presence of other elements, namely yttrium, should not be disregarded, attending to the known influence of rare earth elements (REE) on the electronic properties of other elements.

Figure 2 shows the X-ray diffraction patterns of FA_ZSM5 zeolite samples, along with commercial ZSM-5 zeolite used as reference material.

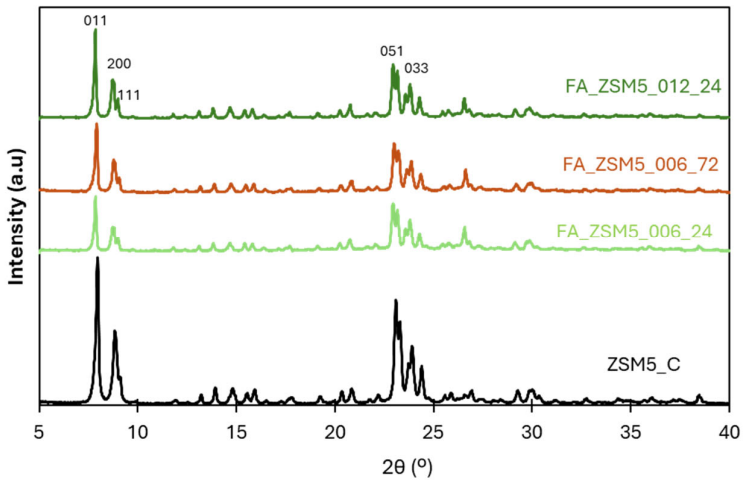

Figure 2. X-ray diffraction patterns of FA_ZSM5 samples and commercial ZSM-5. Miller indexes of the main diffraction peaks are indicated according to the IZA Database of Zeolite Structures (http://www.iza-structure.org/databases/ (accessed on 18 December 2025).

The diffraction pattern of the starting FA material (not shown) presents almost no crystalline phases, with only some low intensity peaks ascribed to silica (quartz), mullite and magnetite [22]. On the other hand, FA-ZSM5 samples preset high intensity peaks typical of a crystalline material. When comparing all FA_ZSM5 samples with the commercial zeolite, ZSM5_C it can be seen that the diffraction patterns are identical. To quantify the crystallinity percentage of the synthesized samples the procedure reported in ASTM D 5758-01 [25] was followed. The crystallinity percentage was obtained by dividing the cumulative area of the selected peaks of each sample by the area correspondent to commercial ZSM-5_C, using Peak-fit 4.12 software (Grafiti Inc., Palo Alto, CA, USA). The results obtained are presented in Table 2. As can be observed, all FA_ZSM5 samples present a high crystallinity percentage of almost 80 %. So, the main conclusion that can be drawn is that the variation of the operating conditions, namely the amount of surfactant added and the duration of the hydrothermal treatment, do not allow the samples to be differentiated.

The N_2 adsorption-desorption isotherms at -196 ^{0}C for FA_ZSM5 samples and reference ZSM5_C are showed in Figure 3. The isotherm and respective textural parameters of FA were not included attending to the very low porosity of the material, but in a previous study the application of the BET method allowed to estimate a specific surface area of 13.2 m^2g^{-1} [22].

 doi:10.20944/preprints202512.2787.v1

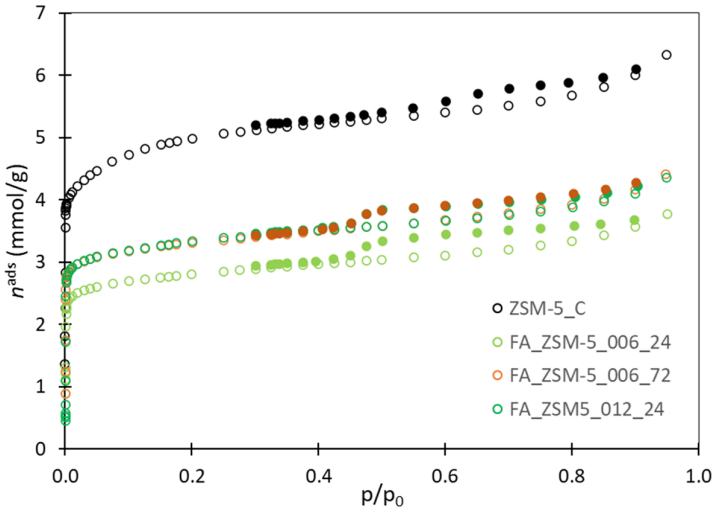

Figure 3. N_2 adsorption-desorption isotherms at -196 ^{0}C for FA-ZSM5 samples and commercial ZSM5_C. The open and closed symbols represent adsorption and desorption, respectively.

All the isotherms displayed in Figure 3 can be classified as a combination of type I+IV [26], showing , as expected, the prevalence of microporosity, as well as some mesoporosity denoted by the presence of hysteresis at relative pressure between 0.5 and 0.95, that can be attributed to particle aggregation. All zeolite samples prepared from FA display a lower microporosity development, when compared to commercial material ZSM5_C, since, in all cases, a notorious downward deviation in the low relative pressure region is noted. The textural parameters for all samples are depicted in Table 2, where the quantification of microporosity was made by applying the α_s method, using a non-porous silica as reference material [27]. This method allows to distinguish the volume of ultramicropores (V_{ulta}, $\phi < 0.7$ nm) and supermicropores (V_{super}, 0.7 nm < ϕ < 2 nm). The volume of the narrow pores, V_{ultra}, is obtained from the line defined by the experimental points determined from $p/p^0 > 0.02$ up to, usually, $p/p^0 = 0.4$, which corresponds to $\alpha_s = 1$. The back extrapolation of the region defined by the points obtained at $p/p^0 > 0.4$ corresponds to the total micropore volume, V_{micro}, allowing to calculate the volume of the larger micropores, V_{super}, through the difference between V_{micro} and V_{ultra}. The mesopore volume, V_{meso}, is obtained by the difference between the total pore volume, V_{total}, and V_{micro}, where V_{total} is the total amount of N_2 uptake at $p/p^0 > 0.95$, in line with the Gurvich rule [27].

Table 2. Degree of crystallinity and textural parameters obtained from N_2 adsorption isotherms for FA_ZSM5 samples, commercial ZSM-5 before (ZSM-5) and after iron loading (Fe/ZSM5_C).

Sample	C_{XRD}[1] (%)	V_{super} ($cm^3\ g^{-1}$)	V_{ultra} ($cm^3\ g^{-1}$)	V_{micro}[2] ($cm^3\ g^{-1}$)	V_{meso}[3] ($cm^3\ g^{-1}$)	A_{ext} ($m^2\ g^{-1}$)
ZSM-5_C	100	0.05	0.10	0.15	0.07	35
FA_ZSM5_006_24	78	0.01	0.07	0.08	0.05	34
FA_ZSM5_012_24	79	0.02	0.08	0.10	0.05	35
FA_ZSM5_006_72	78	0.02	0.08	0.09	0.06	35

[1]Degree of crystallinity (C_{XRD}) calculated from powder X-ray diffraction patterns, using commercial ZSM-5 as reference. [2] Microporous volume, V_{micro}, and external surface area A_{ext}, quantified through the application of α_s method; [3] Mesoporous volume, $V_{meso} = V_{total} - V_{micro}$, where the total volume (V_{total}) corresponds to the amount of N_2 adsorbed at $p/p^o \approx 0.95$.

In line with the previous observations, it can be observed that, for all FA based samples the textural parameters are always lower when compared with the reference ZSM5_C. In general, there are no significant differences between FA_ZSM5 samples, but in more detail, we observe that V_{ultra} is slightly higher in the case of FA_ZSM5_012_24 and FA_ZSM5_006_72 samples, which indicates that the higher amount of TPABr added during synthesis or longer hydrothermal treatment slightly

 doi:10.20944/preprints202512.2787.v1

impact on the development of the narrow pores characteristic of the zeolithic framework. On the other hand, in comparison with the commercial sample, V_{super} is–substantially lower in all cases, whereas V_{meso}, that results mainly from crystallites aggregation, presents slightly lower values for all FA_ZSM5 samples.

To evaluate the electronic properties of the samples the measurements of magnetic susceptibility were performed in a balance, using the configuration of the traditional Gouy method. The mass susceptibility X_g (in c.g.s.) units can be quantified using the general expression:

$$\chi_g = \frac{l}{m}[C(R - R_o)] + \chi_{v,air} \quad (1)$$

(1)

where C is the constant of proportionality of the balance obtained by calibration with a standard substance ($HgCo(SCN)_4$), R is the reading obtained with the tube containing the sample, R_0 is the reading of the empty tube, l is the sample length (cm) m is the sample weight (g), A is the cross-sectional area of the tube and $X_{v,\,air}$ is the volume susceptibility of the displaced air. For powder samples, which is the present case, the term $X_{v,\,air}\,A$, may be ignored. Table 3 presents the values of magnetic susceptibilities for all samples.

Table 3. Magnetic susceptibility (χ_g) measurements for FA_ZSM5 samples and reference ZSM- Fe/ZSM5_C at 25 °C.

Sample	χ_g (×10^5 c.g.s.)
Fe/ZSM5_C	1.4
FA_ZSM5_006_24	5.1
FA_ZSM5_012_24	9.2
FA_ZSM5_006_72	2.9

As expected, all samples present ferromagnetic behavior due to the present of iron in their composition. However, all FA_ZSM5 samples present higher χ_g when comparing the solely iron loaded Fe/ZSM5_C. Since the targeted amount of iron is approximately the same in all samples, the higher χ_g may be attributed to interactions of iron with other elements present on FA. In fact, the influence of REE, particularly Y^{3+} on the magnetic properties of iron containing materials was reported in the literature [28], mentioning that the presence of REE on metal loaded zeolites decreased metal sintering and increases its stability and dispersion, with a positive impact on the hydrogenating activity. [29]. To our knowledge, the effect of yttrium inclusion on heterogenous Fenton catalysts was not yet reported, however, Munoz et al. [30] reviewed several studies where the presence of other elements, such as Mn or Co improved the oxidation rate and mineralization of magnetite-based catalysts due to the accelerated decomposition of H_2O_2 into •OH radicals. Thus, it is reasonable to admit that the presence of yttrium (or traces of other elements, not detected on XPS survey) on FA_ZSM5 samples may have a similar effect.

2.2. Catalytic Tests

The performance of FA_ZSM-5 zeolites was evaluated in the removal of paracetamol (PA) through Fenton reaction at 40 ^{0}C in the presence of H_2O_2. The use of commercial ZSM-5, with only H_2O_2, was assessed as a control test and a negligible PA removal was obtained, leading to the conclusion that, in the chosen operation conditions, the reaction is effective only when Fe species are present.

Figure 4 presents the kinetic curves, expressed as C/C_0 *vs* t where C is the PA concentration for a given reaction time and C_0 is the initial PA concentration, upon reaching the adsorption equilibrium

 doi:10.20944/preprints202512.2787.v1

after 1 h contact between the heterogeneous catalysts and PA molecules. A first inspection shows that the kinetic profiles of all FA_ZSM5 samples show a more pronounced decay of C/C_0 with time, when compared with Fe/ZSM5_C reference sample. Despite these observable differences, a more rational analysis requires the quantification of data though the application of kinetic models.

The kinetic behaviour of the samples was studied using pseudo-first-order and pseudo-second-order kinetic models, assuming that, regardless of the large number of reaction steps, Fenton reaction are described, albeit approximately, by one of these two kinetic models. The pseudo-first-order reaction law assumes that the rate of the reaction depends only on the concentration of one reagent, expressed as:

$$\frac{[C]}{[C_0]} = e^{-k_{p1}t} \tag{2}$$

where $[C]$ is the dye concentration, $[C_0]$ the initial dye concentration, k_{p1} is the pseudo first-order kinetic constant and t is the reaction time. On the other hand, the pseudo-second-order rate law commonly assumes that the reaction rate depends on both reagent and surface sites [31] and can be expressed as:

$$\frac{[C]}{[C_0]} = \frac{1}{k_{p2}[C_0]t + 1} \tag{3}$$

being k_{p2} the pseudo second-order kinetic constant and the other symbols keep the same meaning as stated before.

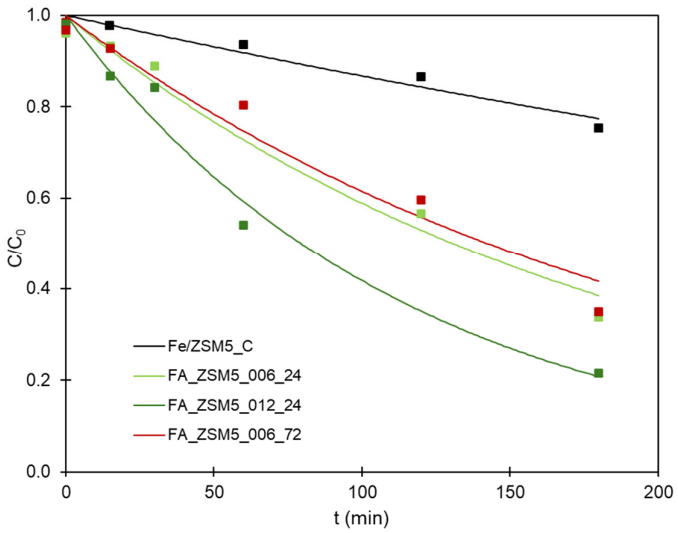

Figure 4. PA removal kinetic curves obtained from the application of pseudo-first-order kinetic model. The points represent the experimental data.

The values of the rate constants of pseudo-first and second order are presented in Table 4. To validate the quality of the fit of nonlinear equations to the experimental points, the following statistical parameters are also present: coefficient of determination (R^2), the fit standard error of the regression (S_{Fit}), the Fisher-Snedecor parameter (F). In all cases, the number of experimental points used in the non-linear regression was five.

 doi:10.20944/preprints202512.2787.v1

Table 4. Rate constants of pseudo-first order (k_{p1}) and pseudo-second-order(k_{p2}) for the kinetic curves of PA removal, correspondent statistical parameters R^2, S_{Fit} and F (see description in the text).

Sample	Pseudo-first order kinetic model			
	k_{p1} (min^{-1})	R^2	s_{Fit}	F
Fe/ZSM5_C	0.0014 ± 0.0002	0.962	0.395	76.4
FA_ZSM5_006_24	0.0053 ± 0.0006	0.979	0.970	137.0
FA_ZSM5_012_24	0.0090 ± 0.0010	0.978	1.190	132.5
FA_ZSM5_006_72	0.0049 ± 0.0007	0.962	1.179	75.4
Sample	**Pseudo-second order kinetic model**			
	k_{p2} (ppm^{-1} min^{-1})	R^2	s_{Fit}	F
Fe/ZSM5_C	0.000087 ± 0.00001	0.949	0.459	55.7
FA_ZSM5_006_24	0.00036 ± 0.0008	0.944	1.562	51.0
FA_ZSM5_012_24	0.0006 ± 0.0001	0.942	1.923	48.9
FA_ZSM5_006_72	0.00033 ± 0.00008	0.918	1.728	33.5

A brief inspection of the results shows that, under the chosen experimental conditions, the pseudo-first-order kinetic model is the one that best fits the experimental data, with the corresponding kinetic constant, k_{p1}, higher when compared with the pseudo-second-order rate constant, k_{p2}. These observations are in line with the literature for other contaminants [32,33] and also in one of the few studies concerning the removal of paracetamol using a heterogenous catalysts [34]. The fitting to the pseudo-first-order model indicates that only the initial phase of the degradation process is occurring since, as can be visualized in Figure 4, a real plateau was never reached even after 180 min reaction.

In line with the analysis of kinetic profiles in Figure 4, the values obtained for rate constants depicted on Table 4 show substantially higher values for all FA_ZSM5 samples when compared with Fe/ZSM5_C. These results cannot be explained by the classic evaluation of crystallinity and texture (Table 2) since in all cases FA_ZSM5 samples present lower crystallinity and V_{micro} when compared with the reference catalyst. To rationalize these results it must be noted that when operating in pH around 4, as in the case of this work, PA molecules may be present in the form of dimers [35,36], with molecular dimensions estimated (in nm) 1.58 (length) × 1.19 (width) × 0.46 (thickness), which are incompatible with the elliptical pore openings of ZSM-5 zeolite (in nm) 0.51× 0.55 and 0.53 × 0.56 [37]. Accordingly, we must consider that the Fenton reactions occur, most likely, at the external surface of zeolite crystals or pore openings.

This assumption justifies the low-rate constant and removal after 180 min. observed in the assay with Fe/ZSM5_C but not the higher values observed when FA_ZSM5 samples were tested. On the other hand, for FA_ZSM5 samples, the structural and textural parameters do not present enough variability to justify the differences between them. However, they all have a fraction of disorganized structure, with about 20% crystallinity lost, where no diffusional constraints are present, which may contribute to the improved catalytic performance when compared with Fe/ZSM5_C. On the other hand, confronting the amount of iron metal ions introduced in Fe/ZSM5_C by IWI (0.8 mmol g^{-1}) with the XPS analysis (0.4 mmol g^{-1}) the low degradation rate for Fe/ZSM5_C sample can be attributed to the inaccessibility of a substantial amount of active sites, which is also in agree with the small decrease of PA concentration after 1 h contact with the samples, indicating low adsorption. The XPS analysis of the representative FA_ZSM5 sample, showed identical amount of iron on the surface, but the presence of yttrium was also detected, which most probably affected the catalytic performance. This assumption is corroborated by sample FA_ZSM5_012_24 that stands out for its superior magnetic susceptibility (Table 3), impacting on the catalytic performance, with k_{p1} almost 1.6 and 1.8 higher than FA_ZSM5_006_24 and 72, respectively and more than 6 times higher than Fe/ZSM5_C sample.

2.3. Lixiviation Tests

To investigate the occurrence of lixiviation effects during PA removal a set of experiments were performed on samples FA_ZSM5_006_72 and FA_ZSM5_012_24 as well as the reference Fe/ZSM5_C.

 doi:10.20944/preprints202512.2787.v1

After the equilibration time of 1 h, the solid was removed by centrifugation and then the reaction was conducted in the usual manner, according to the procedure described ahead. After 45 min the reaction was stopped and the absorbance was measured. In all cases, the ratio between PA concentration after 45 min reaction and the initial concentration, $C/C_0 \approx 1$, meaning that no active species are present in solution after removing the solid, thus heterogenous catalysis is occurring on Fe/ZSM5_C and both FA_ZSM5 samples.

3. Materials and Methods

3.1. Catalysts Preparation

The starting fly-ash (FA) material was composed of the lighter fraction of the ash produced during the combustion of bituminous coal from Colombia in a Portugusese Thermoelectric power plant . The FA sample was taken from the silos that collect the ashes from electrostatic precipitators. Upon analysis, the FA sample was classified as non-compliant for sale, and is therefore considered waste. In this study the FA sample was quartered and used without further treatment. The chemicals used for the zeolite synthesis and catalytic experiments were purchased from Merck (Darmstadt, Germany), and used as received.

The synthesis of ZSM-5 zeolite (MFI structure) was performed according to published protocols [23,24] , with some adaptations. In brief, 1.5 g of FA was suspended in a 2 M NaOH solution at 90 ^{0}C , in a heating plate with temperature control (IKA C-MaHS7, Staufen, Germany). Then, 3.413 g of SiO_2 were added to adjust the global Si/Al ratio to 12 and the required amount of tetrapropylammonium bromide (TPABr) to attain the molar ratio $1SiO_2$: 0.06 or 0.12 TPABr. After 3 h mixing at 210 rpm the suspension was transferred to stainless steel PTFE lined autoclaves and heated at 160 ^{0}C under autogenous pressure for 24 or 72 h. The material was recovered by filtration, washed until pH around 7, dried overnight and clacined at 540 ^{0}C during 5 h, with a heating ramp of 5^0 min^{-1} (Nabertherm B170, Bahnhofstr, Germany) The samples were designated as: FA_ZSM5_x_y, where x is the TPABr added (molar ratio) and y corresponds to the time spent inside the autoclave (h). A commercial ZSM-5 zeolite (Zeolyst, Pennsylvania, EUA), with a SiO_2/Al_2O_3=30 (CBV3024E, Lot2200-99) was used as a reference material, where about 4 wt.% of iron was introduced by incipient wetness impregnation method, using the amount of water correspondent to the previously determined porous volume of the solid. This amount of water was used to dissolve $Fe(NO_3)_3.9H_2O$ (>99%) and mix with the solid until a past was formed. The sample was dried and calcined at 350 ^{0}C, with a heating rate of 5^0 min^{-1}.

3.2. Physicochemical Characterization

The samples were analysed by indunctively coupled plasma - optical emission spectroscopy ICP-AES at Laboratório de Análises, IST, Lisbon, to probe the chemical composition of FA. The surface composition was studied by X-ray photoelectron spectroscopy, XPS, performed at INCAR, Oviedo. The structural characterization of parent FA and produced zeolites was assessed from X-ray powder diffraction (XRD) patterns, acquired at room temperature using a Pan'Analytical PW3050/60X'Pert PRO (θ/2θ) diffractometer (Phillips, Almelo, The Netherlands), equipped with X'Celerator detector with automatic data acquisition (X'Pert Data Collector (v2.0b) software), using a monochromatized CuKα radiation as incident beam, 40 kV-30 mA. The scannings were made in a 2θ range of 5 - 40 ° with a step size of 0.017 ° 2θ and a time per step of 0.6 s. N_2 adsorption/desorption isotherms were performed to characaterize the textural properties of the samples. The assays were made in an automatic apparatus ASAP2010 (Micromerics Instruments Corporation, Norcross, GA, USA). Prior to each experiment the samples (abou 50 mg) were outgassed at 300 °C for 3 h under vacuum better than 10^{-2} Pa. The magnetic susceptibility measurements were performed in a balance MSK-MK1 (Sherwood Scientific, Cambridge, England).

 doi:10.20944/preprints202512.2787.v1

3.3. Catalytic Tests

The catalytic tests were performed following a previously optimized procedure [11]. In brief, 10 mg of the samples was accurately weighted and placed in 50 mL Falcon type tubes. Then, 25 mL of 20 ppm paracetamol (PA) solution was added to each tube and immersed in a thermostatic bath at 40 ºC (Julabo MP, Seelbach, Germany) which was placed on a multiposition magnetic stirrer (Selecta Multimatic 9-S, Barcelona, Spain). The system was left to reach adsorption equilibrium for 1 hour. This equilibrium stage was previously optimized [11] and only after achieving this the reaction was initiated. So, immedately before the reaction begins, the pH was adjusted to a value around 4 using a 0.5 M HCl solution [38]. The reaction started by adding 0.5 mL of a 70 mM H_2O_2 solution to each of the tubes. Then, at pre-determined reaction time the reaction was stopped by adding 3 drops of 0.5 M NaOH solution. The solid was separated from reaction medium by centrifugation (Hermle, Z206A, Gosheim, Germany) and the absorbance of the remaining solution was measured in a double-beam spectrophotometer (VWR, UC-6300PC, Pennsylvania, EUA) using a 10 mm optical length quartz cell and water as reference. At least three individual scans were performed to ensure a standard deviation below 5%. Before the measuremets, a calibration curve was made using PA solutions in concentrations needed to obtain absorbances ranging from 0.15 and 1.0, to obey the Beer-Lambert law.

4. Conclusions

ZSM-5 zeolite was successfully synthesized using fly ash waste, changing the amount of structuring agent and the duration of the hydrothermal treatment. The obtained materials present the diffraction patterns characteristic of MFI zeolite structure, with low impurity content and the N_2 isotherm shows the profile typical of zeolite materials, although the textural parameters are lower when compared with the commercial ZSM-5 zeolite. Beyond the expected Si and Al contents, important amounts of Fe and Y were detected in FA that were incorporated on the synthesized samples. FA-ZSM5 samples showed an increase on magnetic susceptibility when compared with solely iron loaded commercial ZSM-5, disclosing synergistic effects between iron and other elements, such as yttrium, that migrate from FA to the derived zeolite samples. This effect was more expressive for the sample with high amount of structuring agent FA_ZSM5_012_24, which may indicate some influence of the amount of structuring agent on the metal ions distributions, or solely to the heterogeneity of FA raw material. The catalytic performance on the removal of paracetamol though Fenton reaction showed an enhanced removal of PA by FA_ZSM5 samples when compared with Fe/ZSM5_C. This behavior may have two types of interpretations that probably result in a joint effect: i) the catalytic reactions are most likely taking place at the external surface of the zeolite crystals attending that PA molecules tend to organize themselves as dimers that can hardly diffuse into the zeolite pore structure, so the more disorganize structure of FA_ZSM5 samples can in this case benefit the reaction; ii) the presence of yttrium that may enhanced the formation of •OH radicals, which is especially relevant for FA_ZSM5_012_24.

Overall, the preliminary results obtained in this study showed that fly ash waste can be transformed into effective Fenton catalyst without further addition of active sites and no occurrence of lixiviation to the aqueous media. Also, the presence of other chemical elements beyond iron can have a beneficial role in the catalytic performance of the materials.

Author Contributions: Conceptualization, APC and AM; methodology, N.N., H.F.S. and A.S.M.; investigation, N.H. and S.M.; writing—original draft preparation, A.M.; writing—review and editing, A.M. and A.P.C.; supervision, A.M. and A.P.C.; project administration, A.M. All authors have read and agreed to the published version of the manuscript.

Funding: This research was funded by the Fundação para a Ciência e Tecnologia (FCT) through UID/00100/2025, UID/PRR/100/2025 and Instituto Politécnico de Lisboa (IPL) through Project IPL/2024/Ash2ZeoCat ISEL.

Institutional Review Board Statement: Not applicable.

 doi:10.20944/preprints202512.2787.v1

Informed Consent Statement: Not applicable.

Data Availability Statement: Data are contained within the manuscript.

Conflicts of Interest: The authors declare no conflicts of interests.

References

1. Ferreira, I.A.; Carreira, T.G.; Diório, A.; Bergamasco, R.; Vieira, M.F. Occurrence and Removal of Pharmaceuticals from Water Using Modified Zeolites: A Review. *Desalination Water Treat.* **2023**, *302*, 171–183, doi:10.5004/dwt.2023.29762.
2. Całus-Makowska, K.; Dziubińska, J.; Grosser, A.; Grobelak, A. Application of the Fenton and Photo-Fenton Processes in Pharmaceutical Removal: New Perspectives in Environmental Protection. *Desalination Water Treat.* **2025**, *321*, 100949, doi:10.1016/j.dwt.2024.100949.
3. Pacheco-Álvarez, M.; Picos Benítez, R.; Rodríguez-Narváez, O.M.; Brillas, E.; Peralta-Hernández, J.M. A Critical Review on Paracetamol Removal from Different Aqueous Matrices by Fenton and Fenton-Based Processes, and Their Combined Methods. *Chemosphere* **2022**, *303*, 134883, doi:10.1016/j.chemosphere.2022.134883.
4. Nogueira, A.F.; Pinto, G.; Correia, B.; Nunes, B. Embryonic Development, Locomotor Behavior, Biochemical, and Epigenetic Effects of the Pharmaceutical Drugs Paracetamol and Ciprofloxacin in Larvae and Embryos of *Danio Rerio* When Exposed to Environmental Realistic Levels of Both Drugs. *Environ. Toxicol.* **2019**, *34*, 1177–1190, doi:10.1002/tox.22819.
5. Velichkova, F.; Delmas, H.; Julcour, C.; Koumanova, B. Heterogeneous Fenton and Photo-fenton Oxidation for Paracetamol Removal Using Iron Containing ZSM-5 Zeolite as Catalyst. *AIChE J.* **2017**, *63*, 669–679, doi:10.1002/aic.15369.
6. Klavarioti, M.; Mantzavinos, D.; Kassinos, D. Removal of Residual Pharmaceuticals from Aqueous Systems by Advanced Oxidation Processes. *Environ. Int.* **2009**, *35*, 402–417, doi:10.1016/j.envint.2008.07.009.
7. Li, N.; He, X.; Ye, J.; Dai, H.; Peng, W.; Cheng, Z.; Yan, B.; Chen, G.; Wang, S. H2O2 Activation and Contaminants Removal in Heterogeneous Fenton-like Systems. *J. Hazard. Mater.* **2023**, *458*, 131926, doi:10.1016/j.jhazmat.2023.131926.
8. Ganiyu, S.O.; Zhou, M.; Martínez-Huitle, C.A. Heterogeneous Electro-Fenton and Photoelectro-Fenton Processes: A Critical Review of Fundamental Principles and Application for Water/Wastewater Treatment. *Appl. Catal. B Environ.* **2018**, *235*, 103–129, doi:10.1016/j.apcatb.2018.04.044.
9. Domergue, L.; Georgi, A.; Schierz, A.; Cimetière, N.; Giraudet, S.; Hauchard, D. Regeneration of the Adsorption Properties of Hydrophobic Zeolites for the Treatment of Diclofenac by Fenton-like Process: Influence of Fenton Catalyst Location. *Sep. Purif. Technol.* **2025**, *379*, 134557, doi:10.1016/j.seppur.2025.134557.
10. Azusano, I.P.I.; Caparanga, A.R.; Chen, B.H. Degradation of Ketoprofen Using Iron-Supported ZSM-5 Catalyst via Heterogeneous Fenton Oxidation. *IOP Conf. Ser. Earth Environ. Sci.* **2020**, *612*, 012048, doi:10.1088/1755-1315/612/1/012048.
11. Carvalho, A.P.; Costa, J.; Martins, A.; Fonseca, A.M.; Neves, I.C.; Nunes, N. Zeolite Modification for Optimizing Fenton Reaction in Methylene Blue Dye Degradation. *Colorants* **2025**, *4*, 10, doi:10.3390/colorants4010010.
12. Adityosulindro, S.; Julcour, C.; Barthe, L. Heterogeneous Fenton Oxidation Using Fe-ZSM5 Catalyst for Removal of Ibuprofen in Wastewater. *J. Environ. Chem. Eng.* **2018**, *6*, 5920–5928, doi:10.1016/j.jece.2018.09.007.
13. Yao, Z.T.; Ji, X.S.; Sarker, P.K.; Tang, J.H.; Ge, L.Q.; Xia, M.S.; Xi, Y.Q. A Comprehensive Review on the Applications of Coal Fly Ash. *Earth-Sci. Rev.* **2015**, *141*, 105–121, doi:10.1016/j.earscirev.2014.11.016.
14. Gollakota, A.R.K.; Volli, V.; Shu, C.M. Progressive Utilisation Prospects of Coal Fly Ash: A Review. *Sci. Total Environ.* **2019**, *672*, 951–989, doi:10.1016/j.scitotenv.2019.03.337.
15. Vassilev, S.V.; Vassileva, C.G. Methods for Characterization of Composition of Fly Ashes from Coal-Fired Power Stations: A Critical Overview. *Energy Fuels* **2005**, *19*, 1084–1098, doi:10.1021/ef049694d.

 doi:10.20944/preprints202512.2787.v1

16. Anand Rao, K.; Serajuddin, M.; RamaDevi, G.; Thakurta, S.G.; Sreenivas, T. On the Characterization and Leaching of Rare Earths from a Coal Fly Ash of Indian Origin. *Sep. Sci. Technol. Phila.* **2020**, *6395*, doi:10.1080/01496395.2020.1718705.
17. Taggart, R.K.; Rivera, N.A.; Levard, C.; Ambrosi, J.-P.; Borschneck, D.; Hower, J.C.; Hsu-Kim, H. Differences in Bulk and Microscale Yttrium Speciation in Coal Combustion Fly Ash. *Environ. Sci. Process. Impacts* **2018**, *20*, 1390–1403, doi:10.1039/C8EM00264A.
18. Feng, W.; Wan, Z.; Daniels, J.; Li, Z.; Xiao, G.; Yu, J.; Xu, D.; Guo, H.; Zhang, D.; May, E.F.; et al. Synthesis of High Quality Zeolites from Coal Fly Ash: Mobility of Hazardous Elements and Environmental Applications. *J. Clean. Prod.* **2018**, *202*, 390–400, doi:10.1016/j.jclepro.2018.08.140.
19. Zhang, W.; Zhang, T.; Lv, Y.; Jing, T.; Gao, X.; Gu, Z.; Li, S.; Ao, H.; Fang, D. Recent Progress on the Synthesis and Applications of Zeolites from Industrial Solid Wastes. *Catalysts* **2024**, *14*, 734, doi:10.3390/catal14100734.
20. Ndlovu, N.Z.N.; Ameh, A.E.; Petrik, L.F.; Ojumu, T.V. Synthesis and Characterisation of Pure Phase ZSM-5 and Sodalite Zeolites from Coal Fly Ash. *Mater. Today Commun.* **2023**, *34*, 105436, doi:10.1016/j.mtcomm.2023.105436.
21. Lee, Y.-R.; Soe, J.T.; Zhang, S.; Ahn, J.-W.; Park, M.B.; Ahn, W.-S. Synthesis of Nanoporous Materials via Recycling Coal Fly Ash and Other Solid Wastes: A Mini Review. *Chem. Eng. J.* **2017**, *317*, 821–843, doi:10.1016/j.cej.2017.02.124.
22. Rosa, T.; Martins, A.; Santos, M.; Trindade, T.; Nunes, N. Coal Fly Ash Waste, a Low-Cost Adsorbent for the Removal of Mordant Orange Dye from Aqueous Media. *J. Braz. Chem. Soc.* **2021**, *00*, 1–12, doi:10.21577/0103-5053.20210116.
23. Vichaphund, S.; Aht-Ong, D.; Sricharoenchaikul, V.; Atong, D. Characteristic of Fly Ash Derived-Zeolite and Its Catalytic Performance for Fast Pyrolysis of Jatropha Waste. *Environ. Technol.* **2014**, *35*, 2254–2261, doi:10.1080/09593330.2014.900118.
24. Mi, X.; Hou, Z.; Li, X. Controllable Synthesis of Nanoscaled ZSM-5 Aggregates with Multivariate Channel under the Synergistic Effect of Silicate-1 and TPABr Using Dual-Silica Source. *Microporous Mesoporous Mater.* **2021**, *323*, 111224, doi:10.1016/j.micromeso.2021.111224.
25. ASTM D5758-01, 2021. Standard Test Method for Determination of Relative Crystallinity of Zeolite ZSM-5 by X-Ray Diffraction 2021.
26. Thommes, M.; Kaneko, K.; Neimark, A.V.; Olivier, J.P.; Rodriguez-reinoso, F.; Rouquerol, J.; Sing, K.S.W. Physisorption of Gases , with Special Reference to the Evaluation of Surface Area and Pore Size Distribution (IUPAC Technical Report). *Pure Appl. Chem.* **2015**, *87*, 1051–1069, doi:10.1515/pac-2014-1117.
27. Gregg, S.J.; Sing, K.S.W. *Adsorption, Surface Area and Porosity*; Second Edi.; Academic Press: London, 1982; ISBN 0-12-300956-1.
28. Kowalik, P.; Mikulski, J.; Borodziuk, A.; Duda, M.; Kamińska, I.; Zajdel, K.; Rybusinski, J.; Szczytko, J.; Wojciechowski, T.; Sobczak, K.; et al. Yttrium-Doped Iron Oxide Nanoparticles for Magnetic Hyperthermia Applications. *J. Phys. Chem. C* **2020**, *124*, 6871–6883, doi:10.1021/acs.jpcc.9b11043.
29. Martins, A.; Silva, J.M.M.; Ribeiro, M.F.F. Influence of Rare Earth Elements on the Acid and Metal Sites of Pt / HBEA Catalyst for Short Chain n -Alkane Hydroisomerization. *Appl. Catal. Gen.* **2013**, *466*, 293–299, doi:10.1016/j.apcata.2013.06.043.
30. Munoz, M.; De Pedro, Z.M.; Casas, J.A.; Rodriguez, J.J. Preparation of Magnetite-Based Catalysts and Their Application in Heterogeneous Fenton Oxidation – A Review. *Appl. Catal. B Environ.* **2015**, *176–177*, 249–265, doi:10.1016/j.apcatb.2015.04.003.
31. Phan, T.T.N.; Nikoloski, A.N.; Bahri, P.A.; Li, D. Adsorption and Photo-Fenton Catalytic Degradation of Organic Dyes over Crystalline $LaFeO_3$ -Doped Porous Silica. *RSC Adv.* **2018**, *8*, 36181–36190, doi:10.1039/C8RA07073C.
32. Raheb, I.; Manlla, M.S. Kinetic and Thermodynamic Studies of the Degradation of Methylene Blue by Photo-Fenton Reaction. *Heliyon* **2021**, *7*, e07427, doi:10.1016/j.heliyon.2021.e07427.
33. Chen, Y.; Cheng, Y.; Guan, X.; Liu, Y.; Nie, J.; Li, C. A Rapid Fenton Treatment of Bio-Treated Dyeing and Finishing Wastewater at Second-Scale Intervals: Kinetics by Stopped-Flow Technique and Application in a Full-Scale Plant. *Sci. Rep.* **2019**, *9*, 9689, doi:10.1038/s41598-019-45948-9.

 doi:10.20944/preprints202512.2787.v1

34. Van, H.T.; Nguyen, L.H.; Hoang, T.K.; Nguyen, T.T.; Tran, T.N.H.; Nguyen, T.B.H.; Vu, X.H.; Pham, M.T.; Tran, T.P.; Pham, T.T.; et al. Heterogeneous Fenton Oxidation of Paracetamol in Aqueous Solution Using Iron Slag as a Catalyst: Degradation Mechanisms and Kinetics. *Environ. Technol. Innov.* **2020**, *18*, 100670, doi:10.1016/j.eti.2020.100670.
35. Galhetas, M.; Mestre, A.S.; Pinto, M.L.; Gulyurtlu, I.; Lopes, H.; Carvalho, A.P. Carbon-Based Materials Prepared from Pine Gasification Residues for Acetaminophen Adsorption. *Chem. Eng. J.* **2014**, *240*, 344–351, doi:10.1016/j.cej.2013.11.067.
36. Nematollahi, D.; Shayani-Jam, H.; Alimoradi, M.; Niroomand, S. Electrochemical Oxidation of Acetaminophen in Aqueous Solutions: Kinetic Evaluation of Hydrolysis, Hydroxylation and Dimerization Processes. *Electrochimica Acta* **2009**, *54*, 7407–7415, doi:10.1016/j.electacta.2009.07.077.
37. Baerlocher, Ch., Meier W.M., Olson, D.H. *Atlas of Zeolite Framework Types*; 5th Editio.; Elsevier, 2001; ISBN 0-444-50701-9.
38. Aleksić, M.; Kušić, H.; Koprivanac, N.; Leszczynska, D.; Božić, A.L. Heterogeneous Fenton Type Processes for the Degradation of Organic Dye Pollutant in Water — The Application of Zeolite Assisted AOPs. *Desalination* **2010**, *257*, 22–29, doi:10.1016/j.desal.2010.03.016.